Proceedings of the Reactor Physics Asia 2015 (RPHA15) Conference
Jeju,Korea,Sept. 16-18, 2015

The Development of JPTS Code System on Nuclear Reactor Simulation

Deng Li[a,b*], Shi Dunfu[b], Li Gang[a,b], Cheng Tangpei[b], Zhang Baoyin[a,b], Shangguan Danhua[a,b], Ma Yan[a,b], Hu Zehua[a,b], Fu Yuanguang[b], Li Rui[b], Hu Xiaoli[b]
[a] Institute of Applied Physics and Computational Mathematics (IAPCM),
[b] CAEP Software Center for High Performance Numerical Simulation, Beijing, China
[*]Corresponding author: deng_li@iapcm.ac.cn

1. Introduction

The high-fidelity, large-scale simulation of the nuclear reactor must be conducted by High Performance Computing (HPC). Based on programming support infrastructures [1], IAPCM (Institute of Applied Physics and Computational Mathematics) is developing a particle transport code system which can be applied to the time dependent and time independent simulation of nuclear reactor and radiation shielding calculation. The support infrastructures act as a bridge between the application program and the super computer, including JASMIN (J Adaptive Structured Meshes applications Infrastructure), JAUMIN (J Adaptive Unstructured Meshes applications Infrastructure), and JCOGIN (J Combinatorial Geometry Infrastructure).

The particle transport simulation system JPTS includes mainly four codes: JMCT (J Monte Carlo Transport), JSNT (J S_N Transport), JBURN, JNuDa (J Nuclear Data library) and a suit of data library: NuDa (see Fig. 1). Furthermore, the CAD pre-processor JLAMT (J Large-scale Automatic Modeling Tool) and view pro-processor TeraVAP are equipped in the JPTS system. JMCT is a continuous- and multigroup-energy Mont Carlo code. It can calculate neutron, photon and coupled neutron/photon transport. It is developed on the combinatorial geometry infrastructure JCOGIN. JSNT is a parallel 3D discrete ordinates radiation transport code. It is developed both on the adaptive structured and adaptive unstructured mesh infrastructures. JBURN is coupled with JMCT and JSNT to perform the depletion calculation.

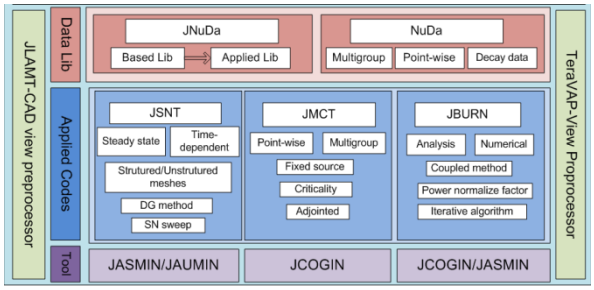

Fig. 1. JPTS particle transport system

2. JMCT, JSNT and JBURN

*2.*1 JMCT

JMCT is a 3-D Monte Carlo neutron, photon and coupled neutron/photon transport code [2]. It is developed on the JCOGIN infrastructure integrating the geometry operation, particle track calculation, domain decomposition, random generator and the parallel computation, mainly written in C, C++ and FORTRAN 95. It can perform both parallel computation of MPI (for particles) and OpenMP (for domains) (see Fig. 2). Both continuous-energy and multi-group energy data libraries, which is produced by JNuDa, can be used in the simulation. It is with the capability to calculate the eigenvalue of the critical system, depletion of the nuclear reactor, the radioactivity of materials under radiation, and the radiation shielding. The model can be built by the CAD modeling tools JLMT [3]. Recently, it can be applied to the full core, pin-by-pin simulation of the commercial nuclear power reactor. The results such as neutron flux, power density can be viewed in 3D pictures in the TeraVAP pro-processor platform. With the given histogram of the reactor, the depletion calculation of the reactor can be conducted. Recently, JMCT can handle the model with more than hundred millions depletion cells. The iteration of soluble boron concentration to yield the desired k_{eff} is implemented into the code as well.

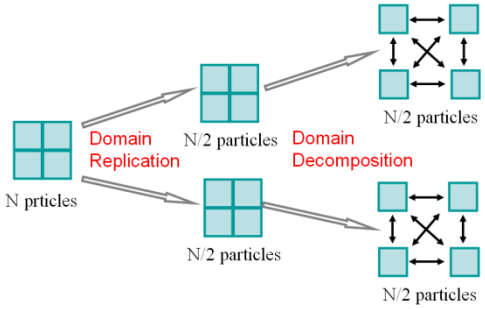

Fig. 2. Domain decomposition and domain replication

2.2 JSNT

JSNT is the generalized name of two deterministic SN transport codes, JSNT-S and JSNT-U. JSNT-S is a parallelizing code developed on JASMIN framework, and JNST-U is a parallelizing code developed on JAUMIN framework. This paper mainly introduces JSNT-S. JSNT-S is a 3D S_N multi-group radiation transport code under active development at CAEP-SCNS (Software Center for High Performance Numerical Simulation, China Academy of Engineering Physics), aiming at high performance simulation of reactor physics and radiation shielding. It is parallelized mainly by domain partition algorithm. The space-angle parallelization scheme based on data-driven for flux sweeping is utilized in the code. The acceleration scheme, e.g. PCR (Partial Current Rebalance) method

with AMG (Algebraic Multi-grid) solver, is implemented into the code as well.

The compute flow of JSNT-S is mainly composed of three phases. The first phase is the data initialization. The second phase is the S_N solve, which is divided into source iterations over energy and flux iterations over space-angle. In the third phase, the overall performance is monitored by the JASMIN time manager and memory utilities, and then the finalization of parallel-computing environment and the result output. In the output data, k-eigenvalue and convergence information are organized in text format, and the cellwise data such as material, scalar flux and response are organized in HDF5 format for data visualization and analysis.

2.3 JBURN

In the reactor physics or radio-activation calculation, the changes of material composition must be taken into account. This is handled by depletion codes. The code solves the first-order linear differential equations:

$$\frac{dN_i}{dt} = -\lambda_i^{eff} N_i + \sum_j^n b_{j,i}^{eff} \lambda_j^{eff} N_j \quad \text{for } i = 1,\ldots,n, \qquad (1)$$

where N_i is the atomic density of nuclide i, λ_i^{eff} is the effective decay constant of nuclide i, and $b_{j,i}^{eff}$ is the effective branching ratio from nuclide j to nuclide i. There are several algorithms to solve the system of decay and transmutation equations in depletion calculation, e.g. Transmutation Trajectory Analysis (TTA), Taylor expansion, Chebyshev Rational Approximation Method (CRAM) [4, 5]. Recently, both TTA and CRAM methods are implement into JMCT. The depletion calculation is paralleled in the reactor simulation as well.

3. Validation and verification

3.1 Simulation of BEAVRS with JMCT

The BEAVRS model was released by MIT Computational Reactor Physics Group in July 7, 2013 [6]. The benchmark provides a highly-detailed PWR specification with two cycles of measured operational data. The reactor is a 4-loop Westinghouse PWR with the thermal power of 3411 MW. In the first cycle, it is loaded with 81.8 MT heavy metal. There are 193 fuel assemblies divided into three regions loaded with the enrichment of 1.6 w/o, 2.4 w/o and 3.1 w/o ^{235}U, respectively (see Fig. 3). Each assembly has 17×17 pins bundled by 8 spacers. There are 264 fuel rods, and other 25 pins are guide tubes, burnable absorber rods and instrument tubes. In the axial direction, the active fuel length is 365.76 cm (see Fig. 4).

The advanced CAD modeling tool JLAMT is applied to build the model. The pins are modeled in details and the spacers are modeled with the suggested configuration. In axial direction, 398 UO_2 pellets are in the region with the coordinate from 36.007 cm (bottom of active fuel) to 401.767 cm (top of active fuel), as shown in Fig. 4. To make sure that the mesh of spacer fully contains the meshes of pellets, the meshes of pellets are not equally divided. There are 25.22 millions of cell in total in the simulation.

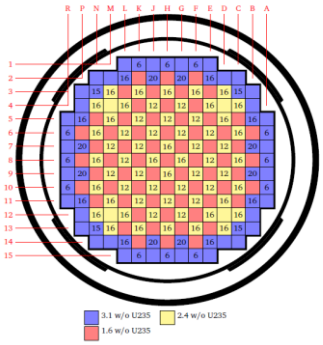

Fig. 3. Core in radial plane

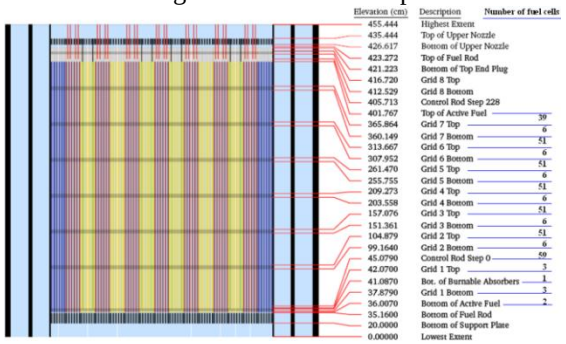

Fig. 4. Scale view of axial cross section and number of fuel cells for axial planes in the active fuel region

The HZP (Hot Zero Power) of the reactor is calculated by JMCT. The evaluated nuclear data library based on ENDF/B-VII is applied in the calculation. Due to the memory consuming, domain decomposition is applied. The space domain is decomposed into 8 parts in 2 (x-direction) ×2 (y-direction) ×2 (z-direction) (see Fig. 5). The domains are generated automatically. Both domain decomposition and domain replication are conduct on 4096 CPU cores, with 8 domain decompositions × 512 domain replications. The calculation is run with 1000 cycles in total and discarding 400 cycles, tracking 81.92 million particles each cycle.

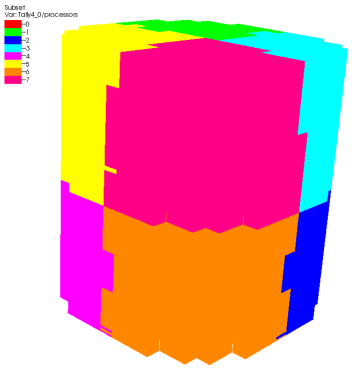

Fig. 5. Domain decomposition (2×2×2)

Table I Max error and min error of flux and energy deposition for all fuel pins

Count	MAX	MIN	95%	99%
Flux	0.0091	0.00118	<0.00332	<0.00423
Energy deposition	0.01933	0.00254	<0.0075	<0.00955

Table II k_{eff} comparison in different control rod statuses and boron concentration [7]

HZP Critical Boron Evaluation	Boron Concentration	JMCT (95% confidence level)	OpenMC (95% confidence level)	MC21 (95% confidence level)
ARO	975	1.000479 ±0.000030	0.99920 ±0.00004	0.9992614 ±0.000004 (average)
D in	902	1.002174 ±0.000030	1.00080 ±0.00004	
C,D in	810	1.001419 ±0.000032	1.00023 ±0.00005	
A,B,C,D in	686	0.9999172 ±0.000032	0.99884 ±0.00004	
A,B,C,D,SE,SD,SC in	508	0.9983806 ±0.000032	0.99725 ±0.00004	

Table III Comparison of control rod worths in different control rod statuses and boron concentration [7]

HZP Bank worth	Boron (ppm)	Measure (pcm)	MC21 (pcm)	OpenMC (pcm)	JMCT (pcm)
D	938.5	788	773	771±6	770±6
C with D in	856	1203	1260	1234±7	1258±6
B with D,C in	748	1171	1172	1197±7	1162±6
A with D,C,B in	748	548	574	556±6	578±6
SE with D,C,B,A in	597	461	544	501±6	543±6
SD with D,C,B,A,SE in	597	772	786	844±6	781±6
SC with D,C,B,A,SE,SD in	597	1099	1122	1049±6	1107±6

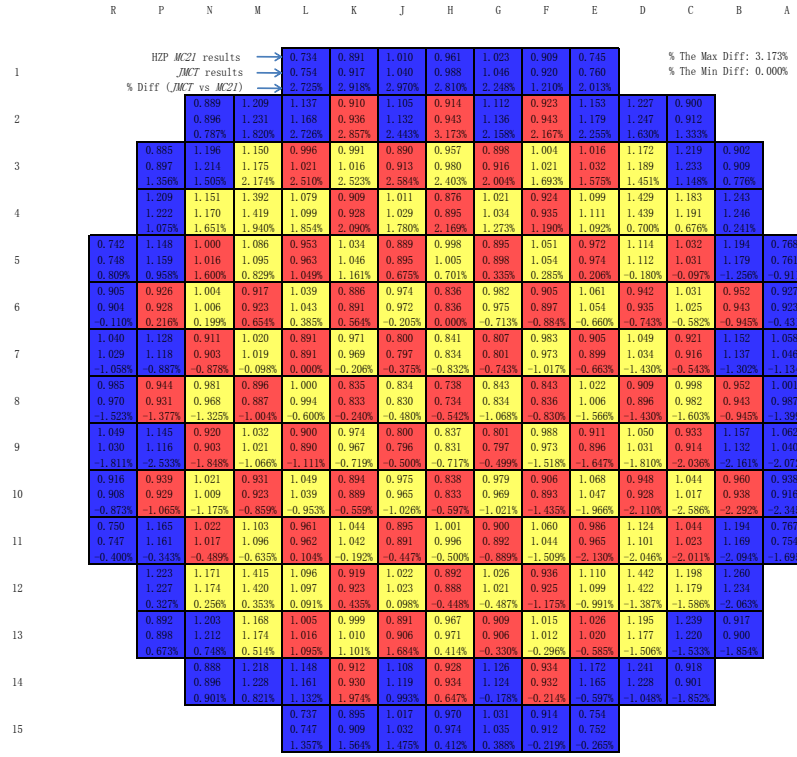

Fig. 6. Comparison of power difference between JMCT and MC21

Table I shows the standard deviation distribution in different confidence level. Table II shows the comparison of k_{eff} to MC21 in different boron concentrations and control rod position. Table III shows control rods values in temperature of 556K. Figure 6 shows the comparisons of power density between MC21 and JMCT in assemblies in the case of all of control rods out (ARO). The maximal Diff is 3.17%, where Diff= (JMCT-MC21)/JMCT. It shows that the results of JMCT are in good agreement with the experimental data and the simulation results of MC21.

3.2 Simulation of VENUS-3 with JSNT-S

The VENUS critical facility is a zero-power reactor with a cruciform-shaped core. The facility was representative of typical irradiation conditions of a modern PWR vessel [8]. Since the model calculation is dedicated to obtain the target quantities for the fast neutron fluxes (neutron energy > 0.1 MeV) and the total iron displacement rates per atom or iron DPA rates, a fixed source calculation is performed using the first 26 fast neutron groups of the BUGLE-96 cross section library (down to the lower energy limit of 0.111 MeV), the S8 order in the flux angular discretization (96 angles) and the P3 order in the expansion of scattering cross section. As depicted in Fig. 7, the cylindrical coordinates with a spatial discretization of 111(R)×113(θ)×71(Z) are employed. The theta-weighted difference approximation is selected for the flux extrapolation. The pointwise flux convergence criterion was set to 1.0E-04. The neutron source distribution, given by OECD/NEA to perform the VENUS-3 benchmark calculations, is expressed in units of fissions per pin per second, arbitrarily normalized to a core averaged power of one fission per second per active fuel pin.

In the VENUS-3 experiment there are 386 dosimeters, which are located at 268 spatial locations. The first investigation is to compare the fast neutron flux above 0.1 MeV at different spatial locations. Fig. 8(a) demonstrates the azimuthal distribution of the fast neutron flux obtained from JSNT-S; and Fig. 8(b), (c) and (d) show the average fast neutron flux calculated by TORT and JSNT-S at different dosimeter. They are in good agreements. In addition, we also investigate the deviation of the equivalent fission fluxes between the computational results and experimental data for different types of dosimeters at different regions. Fig. 9 illustrates the deviation of the 115In(n,n') dosimeters at 104 positions (the inner and outer baffle, the water gap and the barrel), obtained from JSNT-S and NEA/OECD using TORT 3.2 [9]. In both results, It can be found that the deviations of equivalent fission flux are less than 10% at all positions, and the deviation with less than 5% is reached at approximately 90% of the positions.

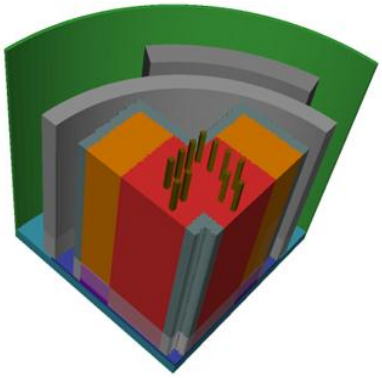

(a)

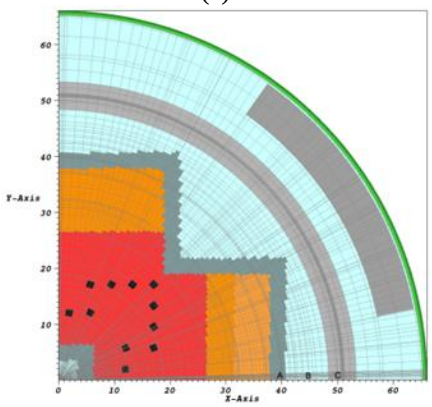

(b)

Fig. 7. Geometry specification for the VENUS-3 benchmark: (a) Core region and steel zones, (b) Horizontal meshes in the (R,θ) plane, section at Z =106.50cm

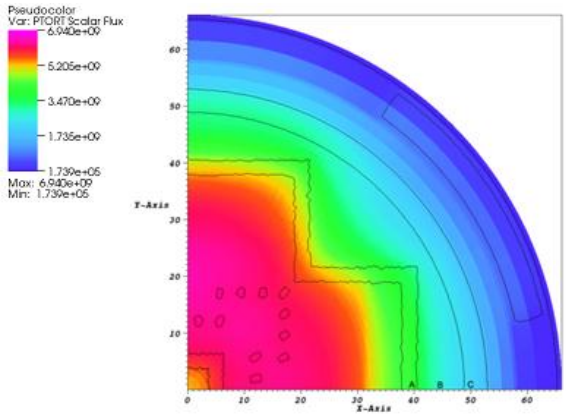

(a)

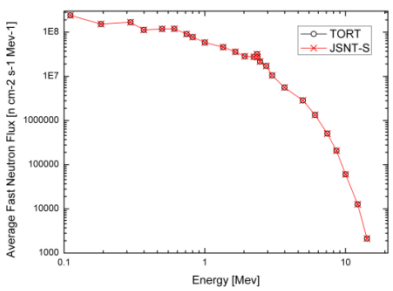

(b)

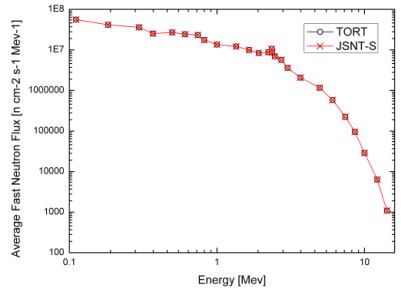

(c)

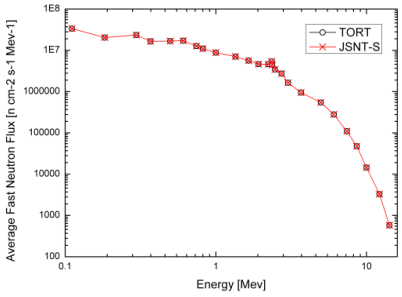

(d)

Fig. 8. (a) Distribution of the fast neutron flux above 0.1 MeV, Z=106.50cm; (b), (c) and (d): Comparison of average fast neutron flux for different energy groups at the dosimeter location A, B and C in (a). locations A, B and C at the outer baffle (39.69, 0.69, 106.50), the water gap (44.73, 0.63, 106.50) and the barrel (49.77, 0.63, 106.50), respectively

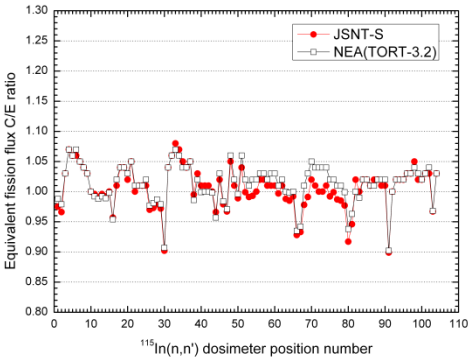

Fig. 9. Deviation of the calculated and measured equivalent fission flux at 104 ^{115}In(n,n') dosimeters positions. The C/E ratio represents the ratio between the computational and experimental results

6. Conclusions

The JPTS particle transport system, especially the parallel algorithm, has been introduced. JMCT is with the capability of the full-core pin-by-pin simulation. The HZP status of the challenging benchmark BEVAUS is calculated. The results agree very well with the experimental data and the simulation results by MC21. The transport with depletion is developed as well. The calculated results will be presented in future.

The parallel radiation transport code JSNT-S, based on JASMIN framework, shows its potential to utilize large-scale parallel machines. It is applied to conduct the radiation shielding simulation of the VENUS-3 facility. It is validated and verified with the experimental data and the simulation results of TORT.

References

1. Mo Z, et al., "JASMIN: a parallel software infrastructure for scientific computing", *Frontiers of Computer Science in China*, 4, 480 (2010).
2. Deng L, Ye T, et al., "3-D Monte Carlo Neutron-Photon Transport Code *JMCT* and Its Algorithms", *PHYSOR 2014*, Kyoto, Japan, September 28 – October 3, 2014.
3. Ma Y, et al., "Pre-Processor Software of 3D MC Particle Transport Code: User's Manual of JLAMT", CAEP-SCNS (2015).
4. Wilson WB, et al., "Class on CINDER'90 CODE and Associated Programs and Data for Transmutation Calculations", Los Alamos National Laboratory, Theoretical Division, Nuclear Theory & Applications Group (T-2), July 14-15, 1998.
5. Isotalo AE, Aarnio PA, "Comparison of Depletion Algorithms for Large systems of Nuclides", *Annals of Nuclear Energy*, 38, 261(2011).
6. "MIT Benchmark for Evaluation And Validation of Reactor Simulations," RELEASE rev. 1.0.1, MIT Computational Reactor Physics Group (2013).
7. Kelly DJ, et al., "MC21 Analysis of the MIT PWR Benchmark: Hot Zero Power Results", *Proceedings of the International Conference on Mathematics and Computational Methods Applied to Nuclear Science and Engineering*, Sun Valley, Idaho, May 5-9, (2013) (CD-ROM).
8. Leenders L, "LWR-PVS Benchmark Experiment VENUS-3 (with Partial Length Shielded Assemblies) – Core Description and Qualification", SCK/CEN, Mol, FCP/VEN/01 (1988).
9. Pescarini M, Orsi R, Borgia M, Martinelli T, "ENEA Nuclear Data Centre Neutron Transport Analysis of the VENUS-3 Shielding Benchmark Experiment", KTSCG-00013, ENEA-Bologna (2001).